Rat cerebral cortical synaptoneurosomal membranes

Structure and interactions with Imidazobenzodiazepine and 1,4-Dihydropyridine calcium channel drugs

J. Moring,[*‡§] W. J. Shoemaker,[*‡§] V. Skita,[‡‖] R. P. Mason,[‡§‖] H. C. Hayden,[‡‡] R. M. Salomon,[§] and L. G. Herbette[*‡¶**]

[*]Alcohol Research Center and [‡]Biomolecular Structure Analysis Center, [§]Departments of Psychiatry and [‖]Radiology, [¶]Medicine and [**]Biochemistry, University of Connecticut Health Center, Farmington, Connecticut 06032; and [‡‡]Department of Physics, University of Connecticut, Storrs, Connecticut 06269 USA

ABSTRACT Small angle x-ray scattering has been used to investigate the structure of synaptoneurosomal (SNM) membranes from rat cerebral cortex. Electron micrographs of the preparation showed SNM with classical synaptic appositions intact, other vesicles, occasional mitochondria, and some myelin. An immunoassay for myelin basic protein placed the myelin content of normal rat SNM at <2% by weight of the total membrane present. X-Ray diffraction patterns showed five diffraction orders with a unit cell repeat for the membrane of 71 to 78 Å at higher hydration states. At lower hydration, 11 orders appeared; the unit cell repeat was 130 Å, indicating that the unit cell contained two membranes. Electron density profiles for the 130-Å unit cell were determined; they clearly showed the two opposed asymmetrical membranes of the SNM vesicles. SNM membrane/buffer partition coefficients (K_p) of imidazobenzodiazepine and 1,4-dihydropyridine (DHP) calcium channel drugs were measured; K_p's for DHP drugs were approximately five times higher in rabbit light sarcoplasmic reticulum than in SNM. Ro 15-1788 and the DHP BAY K 8644 bind primarily to the outer monolayer of vesicles of intact SNM membranes. Nonspecific equilibrium binding of Ro 15-1788 occurs mainly in the upper acyl chain of the bilayer in lipid extracts of SNM membrane.

INTRODUCTION

Our studies of rat cerebral cortical synaptoneurosomal (SNM) membranes (1) were undertaken to test the hypothesis that the location of nonspecific binding of a drug molecule in the cell membrane lipid bilayer is the key to understanding how the drug molecules approach the specific binding site on a membrane-bound receptor.

Our broad interest is in the complex effects of ethanol on brain membranes. Although ethanol does not bind to a specific site in brain membranes, ethanol has a profound effect on chloride ion flux (2). Presumably, ethanol acts through the γ-aminobutyric acid $(GABA)_A$/benzodiazepine receptor complex, which contains a chloride channel and a benzodiazepine binding site as well as binding sites for GABA and picrotoxin. The imidazobenzodiazepine Ro 15-4513, a benzodiazepine receptor partial inverse agonist, can block the effect of ethanol on chloride flux in SNM membranes (3). Ro 15-1788 is a benzodiazepine receptor antagonist which is closely related to Ro 15-4513 (Fig. 1). Because Ro 15-4513 blocks the effects of ethanol on chloride flux, we have chosen to work on it and the related antagonist.

In other work on the effects of ethanol, Littleton and Little (4) and Dolin et al. (5) have shown that the calcium channel associated with the 1,4-dihydropyridine (DHP) calcium channel receptor is involved in developing dependence on ethanol. Symptoms mimicking ethanol withdrawal can be induced by the calcium channel agonist BAY K 8644 (4). Moreover, ethanol withdrawal symptoms can be prevented by administration of DHP calcium channel antagonists (6).

Our ultimate aim is to discover exactly how the imidazobenzodiazepine and DHP drugs interact with their respective receptors and with other components of the SNM, and how acute or chronic administration of ethanol perturbs these interactions. As the first step, using standard methods (7–14) for the analysis of membrane structure by x-ray diffraction, we have investigated the nonspecific equilibrium binding location of BAY K 8644 in the intact membrane, and of Ro 15-1788 in the intact membrane and in a bilayer composed of extracted lipids from SNM membrane. As part of this work, we have determined partition coefficients between SNM membranes and buffer for Ro 15-1788 and for the DHP's BAY K 8644 and nimodipine.

Address correspondence to Dr. J. Moring, Biomolecular Structure Analysis Center, University of Connecticut Health Center, Farmington, CT 06032.

Abbreviations used in this paper: BSA, bovine serum albumin; DHP, dihydropyridine; DPPC, dipalmitoylphosphatidylcholine; DOPC, dioleolylphosphatidylcholine; LSR, light sarcoplasmic reticulum; MBP, myelin basic protein; RBC, red blood cell; SNM, synaptoneurosome.

0006-3495/90/08/513/19 $2.00

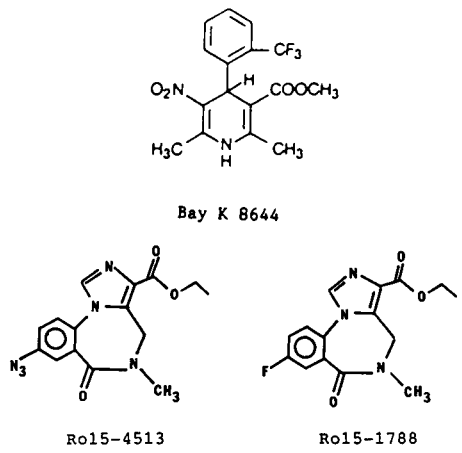

FIGURE 1 Chemical structures of drugs. (*Top*) BAY K 8644, a 1,4-dihydropyridine calcium channel agonist. (*Bottom*) The imidazobenzodiazepines Ro 15-4513, a benzodiazepine receptor partial inverse agonist, and Ro 15-1788, a benzodiazepine receptor antagonist.

METHODS

SNM vesicle preparation

SNM membrane vesicles from rat cerebral cortex were prepared essentially by the method of Hollingsworth et al. (1) with some modifications. The buffer contained 20 mM Hepes, 9 mM Tris, 118 mM NaCl, 4.7 mM KCl, 1.18 mM $MgSO_4$, and 2.5 mM $CaCl_2$, pH 7.4. Any remaining red blood cells (RBC) were removed by centrifugation of the vesicle suspension in an Eppendorf Micro Centrifuge 5415 (Brinkman Instruments, Inc., Westbury, NY) at 3,500 rpm (1000 *g*) for 10 min at 8°C in 1.5 ml polyethylene tubes, after which the portions of the tubes containing the RBC were cut off and the remaining pellets were resuspended in buffer to their original volume. The RBC-free preparation was then lysed in 10 vol of cold distilled deionized water and centrifuged at 5,220 *g* (8,000 rpm) for 10 min at 8°C; the pellet was resuspended in sufficient buffer to restore its original volume. Protein content for each preparation was determined by the method of Lowry et al. (15). Phospholipid concentration was estimated from phosphate content determined by the method of Chen (16).

Membrane multilayer x-ray diffraction samples

Multilayer samples of intact SNM membranes for small-angle x-ray scattering were prepared by centrifuging (L8-55m ultracentrifuge, SW28 rotor, Beckman Instruments, Inc., Palo Alto, CA) a volume of SNM preparation containing 150 μg protein (with or without added drug) at g_{av} = 1,000 (5,000 rpm) for 15 min at 5°C in a lucite sedimentation cell (17) (University of Pennsylvania Biomedical Instrumentation Shop). If a drug was added, BAY K 8644 was added as a 10-mM solution in ethanol; Ro 15-1788 was added as a 1.3-mM solution in the buffer used for making the vesicle suspension (final concentrations before centrifugation and removal of supernatant were 3 mM and 0.65 mM, respectively). If BAY K 8644 was added to a sample, an equal amount of ethanol was added to its control. The pellet was deposited on aluminum foil which was then affixed to a curved glass support (radius of curvature 2.5 cm). The sample was equilibrated over a saturated solution of a salt selected to maintain a given relative humidity and hence a constant hydration state of the multilayer (9).

SNM lipid experiments

Lipids were extracted from SNM preparations after the lysing step by the method of Folch et al. (18), using 2:1 chloroform/methanol at a solvent/sample volume ratio of 50:1. Cholesterol content of the lipid extracts was assayed enzymatically by the method of Heider and Boyett (19) as modified by Chester et al. (20).

Thin films were made in test tubes from the extracted lipids by the method of Bangham et al. (21). The solvent was first dried off under nitrogen while the extract was vortexed. The tubes were then held under vacuum for at least 30 min to remove residual solvent. Vesicles were formed when buffer (2 mM Hepes, 10 mM NaCl) or Ro 15-1788/buffer solution was added to the tubes as they were being vortexed under nitrogen. The final concentration of Ro 15-1788 in the vesicle suspension was 0.5–0.8 mM.

Lipid multibilayer samples for x-ray diffraction were then made by pipetting a volume of vesicle suspension sufficient to contain 150 μg lipid into a lucite sedimentation cell (17) (University of Pennsylvania Biomedical Instrumentation Shop) and centrifuging the vesicles onto aluminum foil at g_{av} = 81,000 (25,000 rpm) for 1 h at 5°C in a Beckman Instruments, Inc. L8-55m ultracentrifuge (SW28 rotor). The supernatant was removed immediately after centrifugation. The pellet was mounted on a curved glass support (radius of curvature 2.5 cm) for x-ray diffraction and allowed to equilibrate over a saturated solution of a salt selected to maintain a given relative humidity.

Other multilayer diffraction samples of extracted lipids were made by the "spin-dry" technique by a variation (22) of the method of Clark et al. (23), in which all volatile fluids in the sample are evaporated completely by the centrifuge vacuum system during sedimentation. The final composition of the sample can be precisely controlled in this way. The lipid vesicle suspension (150 μg lipid) is first subjected to a prespin at 3°C at g_{av} = 81,000 (25,000 rpm) for 30 min (lucite sedimentation cell, Beckman Instruments, Inc. L8-55m, ultracentrifuge, SW28 rotor, 2 ml water cushion in buckets). For the dehydration step, caps which have a 100-μm pinhole are used on the buckets (no water cushion). Centrifugation under vacuum at g_{av} = 30,000 (15,000 rpm) at 3°C for 3½–5 h is sufficient to dehydrate the 50 λ samples completely. In some experiments Ro 15-1788 was added during the formation of the lipid vesicles as explained above, except that the drug was added to the buffer from a 10-mM ethanol stock solution before the drug/buffer solution was added to the thin lipid film. The final amount of the drug in the diffraction samples was 1 mol drug/30 mol lipid.

X-ray diffraction

Diffraction data were collected using an Elliot GX18 rotating anode microfocus generator (Marconi Avionics) supplying Cu K_α radiation (λ = 1.54 Å) in conjunction with a fixed geometry beamline consisting of a single Franks mirror providing line focus at the detection plane, vertical and horizontal limiting slits, a nickel filter, the curved specimen, a tungsten beamstop, and electronic detection. The beam height at the specimen was ~ 1 mm. Data collection was carried out with a Braun one-dimensional position-sensitive proportional counter (Innovative Technology, Inc., Newburyport, MA). Data were transferred to a VAX 8200 (Digital Equipment Corporation, Maynard, MA) for reduction and analysis.

For data on extracted lipids, diffraction orders were integrated by summing the x-ray counts between channels judged to be within the background region on either side of the order, and subtracting a trapezoidal background area determined by applying a linear fit to the

background on either side of the order. A linear s-correction was made to correct for differences in beam geometry at various regions of the curved sample. Intensities were phased by the swelling method (24) using a range of relative humidities from 84% to 98%. Structure factor plots were constructed. Because the unit cell for the extracted lipids must be centrosymmetric, all phases were either 0 or π. The higher orders for which the phases were uncertain were phased by calculating electron density profiles for all of the possible phase combinations and selecting the set of phases which gave a reasonable bilayer profile.

Reduction of data collected on intact membrane multilayer samples at relative humidities higher than 84% (unit cell $d \sim 72$ Å) was similar to that for extracted lipid data. Centrosymmetry was assumed and phases were obtained in the same manner as for lipid data. A modification of the method used by Blaurock and King (13) was used to ascertain that the phases were close to those for a centrosymmetric unit cell. The phase of the first order was fixed at π; phases of other orders were varied as follows: second order, $\phi_2 = \pi + n\pi/8$, $n = 1, 2, \ldots, 8$; fourth order, $\phi_4 = \pi + n\pi/8$, $n = 0, \pm1, \pm2, \ldots, \pm8$. The third order is either very small or equal to zero in these data sets; it was assigned an intensity of zero. Electron density profiles were calculated using each phase of the second order combined with each phase of the fourth order in turn. Structure factor moduli were calculated from these electron density profiles and compared with those derived from the swelling studies.

For diffraction data with a d-spacing of ~130 Å (relative humidity ≤84%), a sum of exponentials was fitted to the background region and subtracted. Diffraction orders were integrated by summing the x-ray counts between what were judged to be the limits of each peak. Linear s-corrections were made to correct for differences in beam geometry at various regions of the curved sample. Box refinements were carried out using the method of Stroud and Agard (25). The multilayer and unit cell Patterson functions were calculated (assuming centrosymmetry) and direct deconvolution of the unit cell Patterson was carried out as described by Lesslauer et al. (26) and Schwartz et al. (27). The Fourier transform of the resulting electron density profile was calculated and sampled at intervals of h/d ($h = 1, 2, \ldots, 11$) ($d = 130.7$ Å) to obtain phases for a centrosymmetric unit cell. These phases were then used with the experimental intensity data to calculate an electron density profile for the 130-Å unit cell.

X-Ray scattering from dispersions of membrane vesicles was carried out using either a point-focus beam (Searle x-ray camera with two Franks mirrors; Baird and Tatlock, Romford, England) or a line focus beam (single Franks mirror) with the beam height set equal to the beam width. Dispersions of lysed SNM in buffer with protein concentrations of ~10–14 mg/ml were sealed in quartz capillaries (1.5 mm i.d.) and exposed to the x-ray beam for periods from 18 h to 3 d. Data were recorded on film. Films were scanned on a Zeineh model SL-2DUV soft laser densitometer (Biomed Instruments, Inc., Fullerton, CA); data were transferred to a VAX 8200 computer system (Digital Equipment Corporation, Maynard, MA) for reduction and analysis. Background was removed by exposing a blank (capillary filled with buffer) to the x-ray beam for the same length of time and subtracting the blank from the data.

Electron microscopy

Samples of original, RBC-free, and lysed SNM preparations were prepared for thin sectioning for transmission electron microscopy by centrifugation in an Eppendorf microcentrifuge for 5 min at 1000 g (3,500 rpm) at 8°C. The pellets were fixed first in 2% glutaraldehyde/1% tannic acid/100 mM sodium cacodylate buffer, pH 7.2, for 1.5 h and given three 15 min washes in sodium cacodylate buffer. The pellets were then fixed in 2% osmium tetroxide/100 mM sodium cacodylate pH 7.2, washed as above, and dehydrated through 50, 70, 90, 95, and 100% ethanol at 30 min per step. After two 30 min washes in propylene oxide, the pellets were agitated overnight in capped vials in 1:1 Polybed 80/propylene oxide. The resin was changed three times the next day and agitated again overnight. The pellets were then placed in a mold in a 60°C oven for 2 d. Sections were made using a Sorvall MT2B microtome (Dupont Instrument Systems, Wilmington, DE) with a diamond knife. Silver sections (80 ± 10 nm) were immersed for 20 min in 2% uranyl acetate, washed, and finally immersed for 20 min in Reynolds lead citrate.

Immunoassay for myelin basic protein

A quantitative immunoassay for myelin basic protein was carried out by a method based on the Western blot. Mouse 14 kDa myelin basic protein (MBP) was used as the standard. Six serial dilutions (1:2) in 0.5 mM Tris, 5% wt/vol sodium dodecyl sulfate, pH ~8 (dilution buffer), of the samples and standard were made. The solutions were adsorbed on Immobilon PVDF Transfer Membrane (Millipore Corp., Bedford, MA) contained in a 96-well filtration apparatus (Schleicher and Schuell, Inc., Keene, NH). Before blotting, the Immobilon had been equilibrated in dilution buffer. After blotting, the membrane was rewetted in methanol for 1–2 s and briefly rinsed with water. The remaining protein sites were blocked by incubating in blocking buffer composed of 5% (wt/vol) bovine serum albumin (BSA) in tris buffered saline (TBS) (10 mM Tris/HCl pH 7.4, 0.9% NaCl) at 37°C for 1 h with gentle agitation. The blot was rinsed four times with wash solution (0.1% [wt/vol] BSA in TBS). The blot was then incubated with primary antibody (polyclonal rabbit α MBP) which had been diluted 1:200 with antibody incubation solution, for 2 h at room temperature with gentle agitation. Antibody incubation solution is 1% BSA (wt/vol), 0.05% (vol/vol) Tween-20 in TBS. The blot was rinsed four times (all rinses in this procedure are 5 min each) with wash solution, then incubated for two h at room temperature with the secondary antibody (goat α-rabbit IgG, horseradish peroxidase conjugated) diluted 1:500 in antibody incubation solution. The blot was rinsed four times with wash solution, then incubated with the horseradish peroxidase substrate 4-chloro-1-naphthol solution as follows: 30 mg 4-chloro-1-naphthol (Sigma Chemical Co., St. Louis, MO) was dissolved in 10 ml methanol which had been cooled to −20°C. This solution was kept at −20°C. First 50 ml TBS and then 30 μl of 30% hydrogen peroxide (Sigma Chemical Co.) were mixed with this solution just before the blot was ready for staining. The substrate solution was mixed for 1 min and then added to the blot immediately after the blot had been removed from the wash solution. The blot was incubated with the substrate solution at room temperature with constant agitation for ~10 min until the degree of staining was appropriate relative to the background color. The staining reaction was stopped by rinsing in water followed by drying the blot. The blot was dried between sheets of blotting paper and stored away from light. It was scanned using a Zeineh model SL-2DUV soft laser densitometer (Biomed Instruments, Inc., Fullerton, CA).

Partition coefficient measurements

Filtration method

Partition coefficients of imidazobenzodiazepine and DHP drugs into intact SNM membranes were experimentally measured using vacuum filtration as previously described (28). The filtration method was selected for this study because of its ability to separate rapidly and efficiently membrane-bound radioligand from free radioligand. Filtration was accomplished using a Brandel cell harvester (Brandel, Inc., Gaithersburg, MD). Using vesicles radiolabeled with ^{14}C-DOPC, we

were able to measure accurately the amount of membrane phospholipid retained on the filter during the filtration process.

To obtain total nonspecific binding, the filters for these experiments were not washed. Reaction mixtures containing drug, but no membrane, were used to correct the total nonspecific binding for binding of drug directly to filters. All filters were counted for radioactivity. The amount of drug in the filtrate was determined by subtracting the number of moles of drug bound to the membrane from the total number of moles of drug added to the reaction mixture. This information, along with the total number of moles of drug in the reaction mixture and the amount of lipid present, corrected for the recovery of membrane on the filters, allowed membrane/buffer partition coefficients to be calculated for each trial.

The concentration of phospholipid in the incubation reaction mixture was fixed at 25.6 μM (20 μg/ml). Radiolabeled drug was added to vesicles of intact membrane to produce a final concentration of drug in the reaction mixture of 2.5×10^{-10}M to 1.88×10^{-7} M. Membrane/buffer partition coefficients were calculated using the following equation: K_P = (grams of drug bound to membrane/grams of membrane phospholipid)/(grams of drug in supernatant/grams of buffer).

Centrifugation method

Partition coefficients of DHP drugs between light sarcoplasmic reticulum (LSR) membrane and buffer were determined by a centrifugation method. SNM membrane vesicles were suspended (12 μg/ml) in a pH 7.3 buffer (10 mM Tris, 150 mM NaCl) containing a known concentration of ^{3}H-labeled drug (28). The samples were centrifuged in polyethylene microcentrifuge tubes (400 μl) in a Beckman Instruments, Inc. SW28 swinging bucket rotor for 1 h at g_{av} = 81,000 (25,000 rpm) at 5°C. Control tubes contained the same reaction mixtures, but were not centrifuged. The tips of the centrifuge tubes containing the membrane pellets were cut off, blotted dry, and placed in scintillation fluid to be counted for ^{3}H radioactivity. The total pellet counts (centrifuged membranes) were corrected by subtracting the counts from blank controls (same size tip of tube which contained uncentrifuged reaction mixture) to give the counts due to drug associated only with membranes. To account for the labeled drug remaining in the supernatant, a 20-μl aliquot was taken from the supernatant in each centrifuge tube; then the tubes were drained, cut, and assayed for radioactivity. All labeled drug added to each tube could be accounted for as distributed among the centrifuged pellets, the walls of the tube, and the supernatant.

Membrane partition coefficients were calculated as above. The amounts of drug in the pellets (bound to membrane) and in the supernatants were determined as described above. The amounts of lipid were corrected for the recovery of membrane in the pellets after centrifugation.

RESULTS

Characteristics of the SNM preparation

Protein contents of the original rat SNM preparations ranged from 11.8 to 21.4 mg/ml. The corresponding phospholipid contents ranged from 12.7 to 18.1 μmol/ml. The highest phospholipid/protein ratio was 1.08 and the lowest 0.74 μmol/mg. For the RBC-free unlysed and lysed preparations, the concentrations were somewhat lower. Electron micrographs of some original, RBC-free unlysed, and lysed samples all showed SNM images with classical synaptic appositions intact, other vesicles, occasional mitochondria, and some nerve myelin (Fig. 2).

An immunoassay for myelin basic protein showed that <2% by weight of the total membrane present in both the lysed and unlysed SNM preparations was myelin. X-Ray scattering experiments on dispersions of rat SNM membranes vesicles showed no Bragg scattering corresponding to *d* spacings of ~150–160 Å, the spacing that would be expected for intact myelin (24). The films showed a weak ring of Bragg-like diffraction (*d* spacing = 76 Å); this could be attributable to a myelin-like multilayer structure.

Characteristics of shiverer mouse SNM

To show that the diffraction was not due to nerve myelin, SNM preparations were made from myelin-free shiverer mice. These mice, which are homozygous for the *shi* mutation, make little or no myelin basic protein and therefore do not form well-ordered myelin (29). The phospholipid/protein ratio was 1.3 μmol/mg for both the RBC-free unlysed and lysed mouse SNM preparations. Electron micrographs were similar to those of the rat SNM preparations, except for an almost total lack of well-ordered myelin (Fig. 3). No myelin at all was detected by an immunoassay for myelin basic protein in either shiverer mouse SNM or whole brain homogenate.

Diffraction from intact SNM membranes

Relative humidities from 98% to 76% were used for the membrane diffraction experiments, but not all of these humidities gave useful results. The highest quality diffraction was obtained at relative humidities of 91%, 87%, and 84%. Although electron micrographs of lysed and unlysed rat SNM preparations appeared similar, the diffraction patterns were different. Unlysed samples generally showed fewer diffraction orders than lysed samples, and the peaks were broader, although the *d* spacing was about the same. Therefore, only lysed preparations were used for diffraction after the preliminary experiments were finished. Most preparations yielded five sharp diffraction orders at relative humidities above 84%. A typical diffraction pattern is shown in Fig. 4. Patterns which were chosen for further analysis were those having relatively sharp, symmetrically shaped peaks with the intensity between the peaks as near as possible to background level. Patterns having extra peaks which did not index, patterns having very broad peaks (due to disorder in the sample), and patterns having split peaks or peaks with shoulders (indicating phase separation) were rejected.

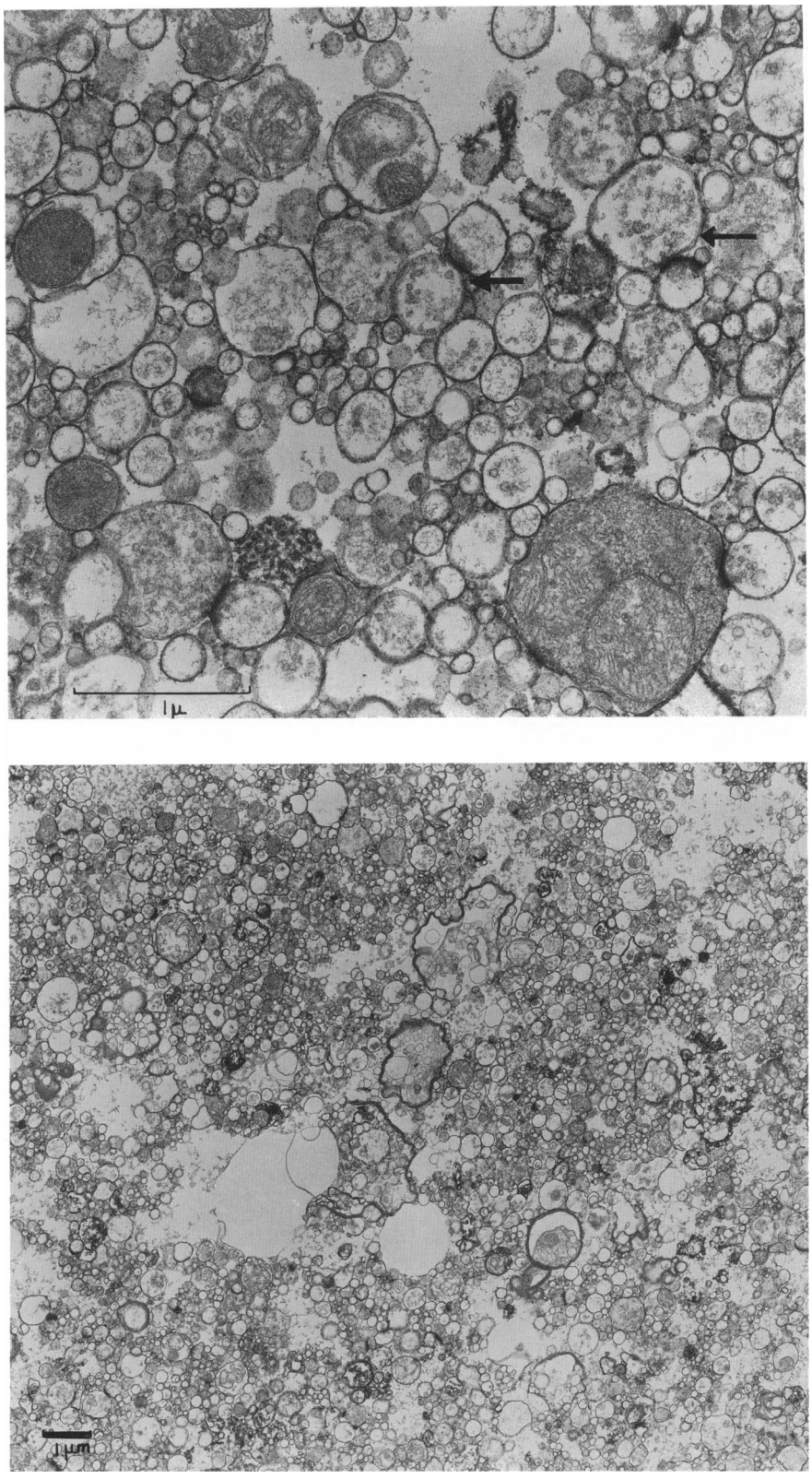

FIGURE 2 Electron micrographs. Rat cerebral cortical SNM preparations. (*a*) Unlysed, two synaptoneurosomes are marked by arrows. (*b*) Lysed, at lower magnification. Note myelin.

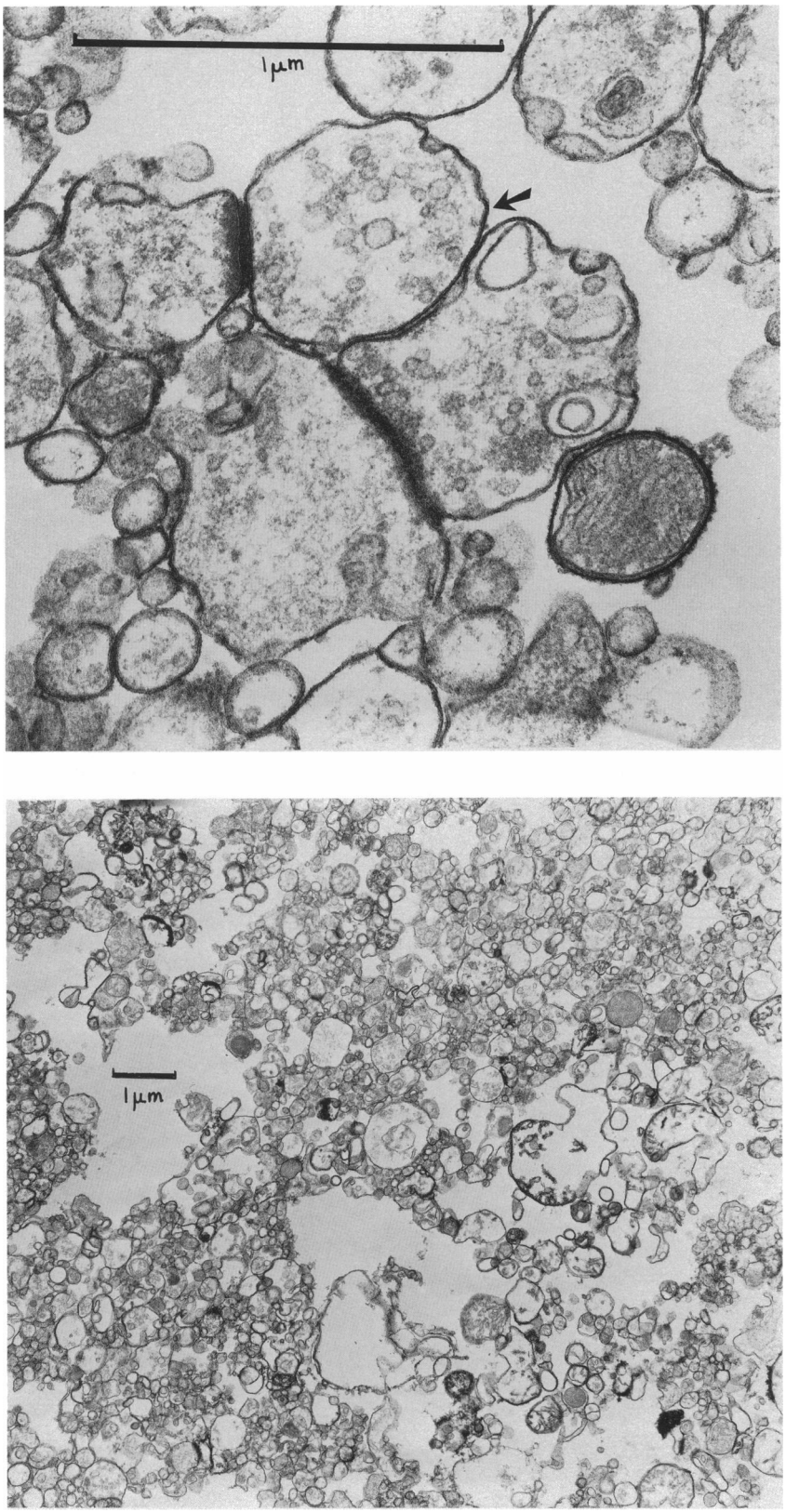

FIGURE 3 Electron micrographs. Shiverer mouse cerebral cortical synaptoneurosome preparations. Note lack of myelin. (*a*) Synaptoneurosomes from unlysed preparation at high magnification. The outer leaflet of the membrane is more densely stained than the inner leaflet, e.g., in the region indicated by the arrow. (*b*) Lysed.

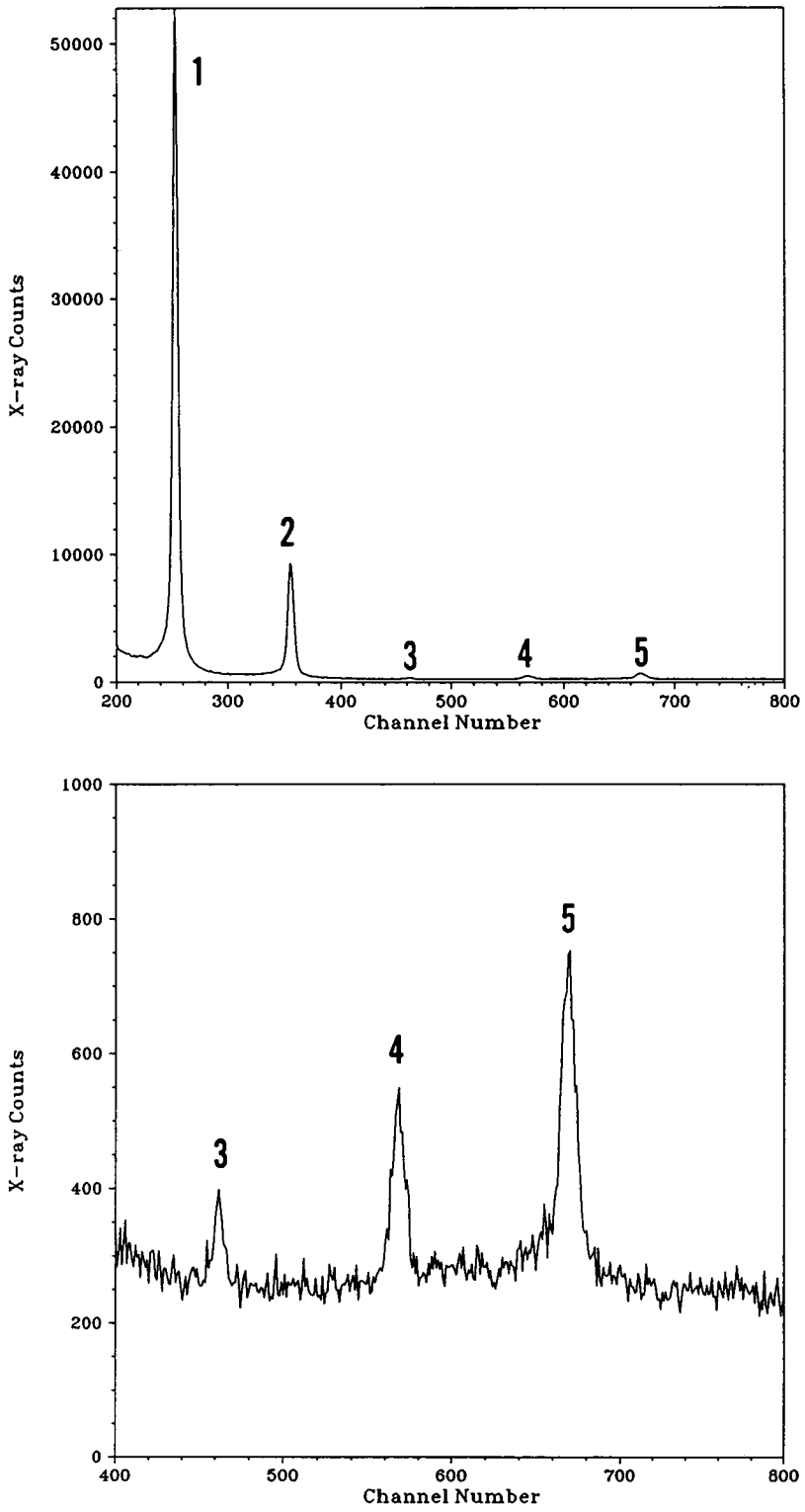

FIGURE 4 X-Ray diffraction patterns from a typical rat cerebral cortical synaptoneurosome preparation at 91% relative humidity and 11.0°C (d = 73.3 Å). The diffraction orders are numbered. Data are shown before Lorentz and background correction. (*a*) Diffraction from lysed preparation. (*b*) Orders 2–5 of the diffraction pattern scaled up.

Diffraction patterns, d spacings, and calculated electron density profiles for the shiverer mouse SNM preparations were similar to those found for rat SNM preparations. Centrosymmetric electron density profiles and d spacings obtained from the shiverer mouse preparations were indistinguishable from those from rat SNM preparations. The results of the diffraction experiments on shiverer mouse SNM indicated that the diffraction from the rat SNM preparations was not due to myelin.

For diffraction patterns recorded at relative humidities above 84%, a modification of the phasing method used by Blaurock and King (13) (see Methods) indicated that the phases are close to those for a centrosymmetric unit cell. The phase of the second order, ϕ_2, must be within $\pm\pi/4$ of ϕ_1. Experiments using x-ray scattering from dispersions of SNM vesicles produced no data beyond 0.026 $Å^{-1}$, a value corresponding to the location of the second order of Bragg diffraction. These data were not good enough to be useful for determining phases. For these reasons phases determined from a swelling study were used to calculate centrosymmetric electron density profiles only for comparison purposes. These electron density profiles were characteristic of a typical membrane bilayer with protein contribution and with d spacings of 71–78 Å, depending on relative humidity. The scattering films also showed a weak ring of Bragg-like diffraction at a d spacing of 76 Å; this would be due to multilamellar vesicles or multilamellar fragments of membrane, possibly myelin (11).

At 84% relative humidity, additional peaks appeared, doubling the d spacing (~130 Å). The doubling was reversed upon raising the relative humidity; therefore no permanent change in the membrane structure had occurred. A diffraction pattern at 84% relative humidity is shown in Fig. 5. At 76% relative humidity, additional small peaks appeared which had lattice spacings different from that of the membrane, indicating phase separation. The pattern at 84% relative humidity represents diffraction from a new unit cell with a repeating unit consisting of two membranes (see Discussion).

Because of the change in structure between 87% and 84% and the phase separation at 76%, it is impossible to do an extensive swelling study to determine phases for the double membrane diffraction pattern. However, other analyses indicate that this diffraction is due to a centrosymmetric unit cell containing two membranes, for which another method of phase determination can be used. The multilayer Patterson function for the diffraction pattern at 84% relative humidity is shown in Fig. 6 *a*; its repeat distance is 130 Å. Correlations are observed between sets of high electron density regions (headgroups) at 65 Å, low electron density regions (methyl troughs) at 65 Å, and between headgroups and methyl troughs at 32.5 Å; these correlations indicate a unit cell containing two membranes. The multilayer Patterson decays within 1250 Å; the envelope is nearly linear in the region from 0 to 2 d. Because the decay indicates that there is disorder in the sample and because the Patterson function approaches zero after about eight repeating units, the box refinement technique is suitable for determining an electron density profile (25). An exhaustive series of box refinements using several types of trial functions and various box sizes was carried out. Best results were obtained from a trial function constructed from many repeats of an electron density profile obtained by the direct deconvolution methods described below. The constructed "multilayer" was multiplied by a half Gaussian to simulate increasing disorder. The trial function and the resulting electron density profile are shown in Fig. 7. The optimal box size was 1,000 Å, although box sizes from 800 to 1,200 Å were suitable. Results from other types of trial functions (boxes, cosines, sums-of-cosines, etc.) were similar. The box refinements yielded electron density profiles characteristic of multiple repeats of a unit cell containing two membranes: a repeat distance of ~130 Å, peaks corresponding to headgroups separated by ~65 Å, and troughs separated by ~65 Å. The distances between the centers of mass of the peaks varied by at most ±4 Å from 65 Å; most refinements gave peak-to-peak distances within 2 Å of 65 Å. These distances indicate that the unit cell is nearly centrosymmetric.

To determine phases for the two-membrane unit cell data, a unit cell Patterson function (Fig. 6 *b*) was calculated from the multilayer Patterson. Direct deconvolution of the unit cell Patterson function (26, 27) yielded an electron density profile characteristic of a double membrane (Fig. 8). The direct deconvolution technique tends to generate large errors, but we used the method only for the purpose of generating sets of phases. Phases obtained by sampling the Fourier transform of this profile at intervals of h/d ($h = 1, 2, \ldots 11$) were applied to the experimentally determined intensity data to calculate an electron density profile for a centrosymmetric unit cell (Figs. 9 and 10). Error analysis as conducted for the extracted lipid preparations, below, could not be done because a swelling series was impossible. The errors in the double membrane electron density profiles, however, are unlikely to be larger than ±5% at any point in the profile.

SNM extracted lipid preparations

The diffraction patterns for the extracted lipids showed six orders, and the electron density profile had a typical bilayer structure (Fig. 11 *a*). When Ro 15-1788 was added to vesicles of extracted SNM lipids prepared by the "spin-dry" method (22), comparison of the electron density profile at 84% relative humidity with that of lipids without added drug showed an increase in electron

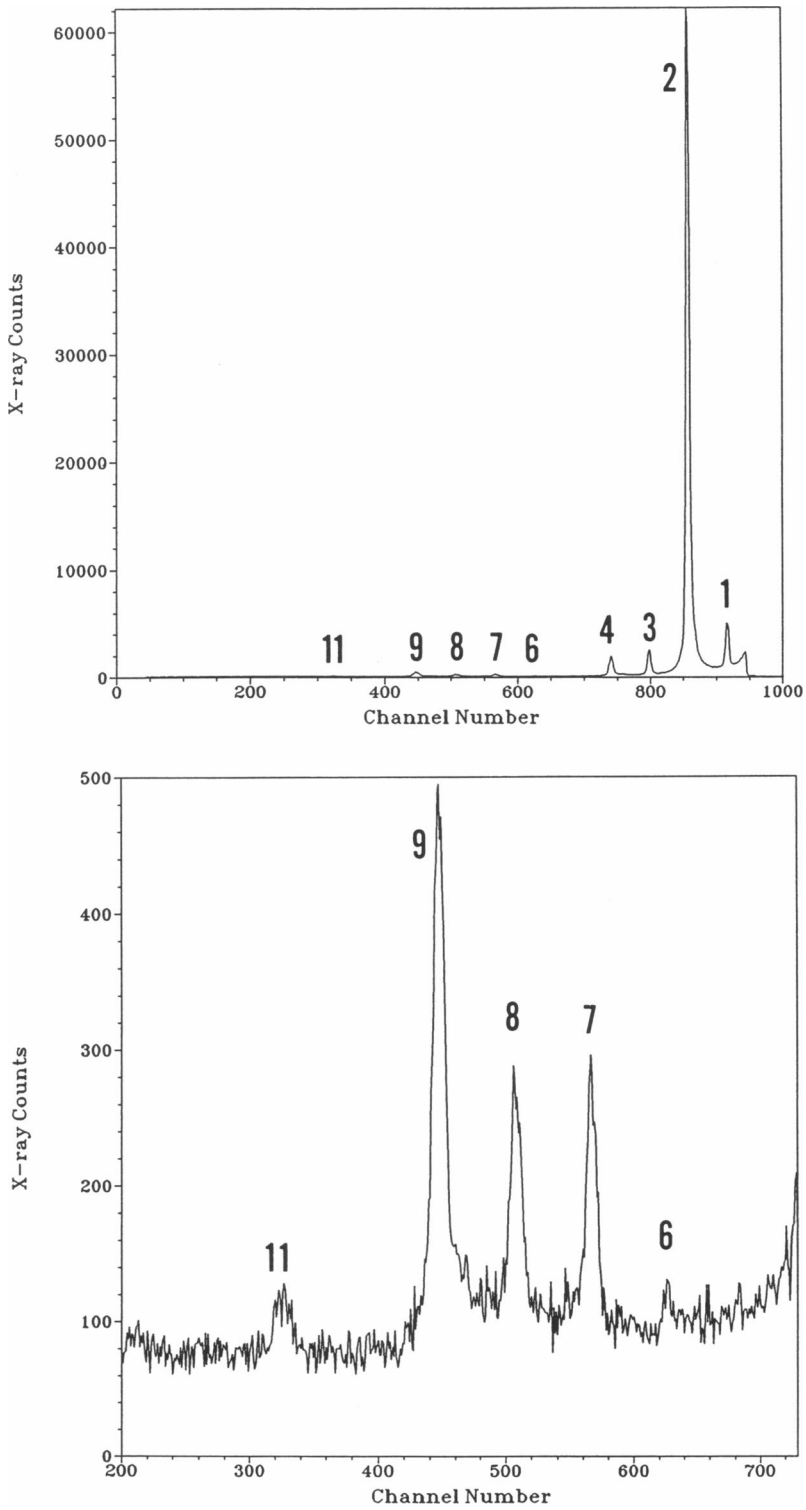

FIGURE 5 X-Ray diffraction pattern from rat synaptoneurosomes. (*a*) Diffraction pattern at 84% relative humidity, 10°C, $d = 130.7$ Å. Data are shown before Lorentz and background correction. The pattern is due to a unit cell containing two membranes. (*b*) Diffraction orders 5–11 scaled up.

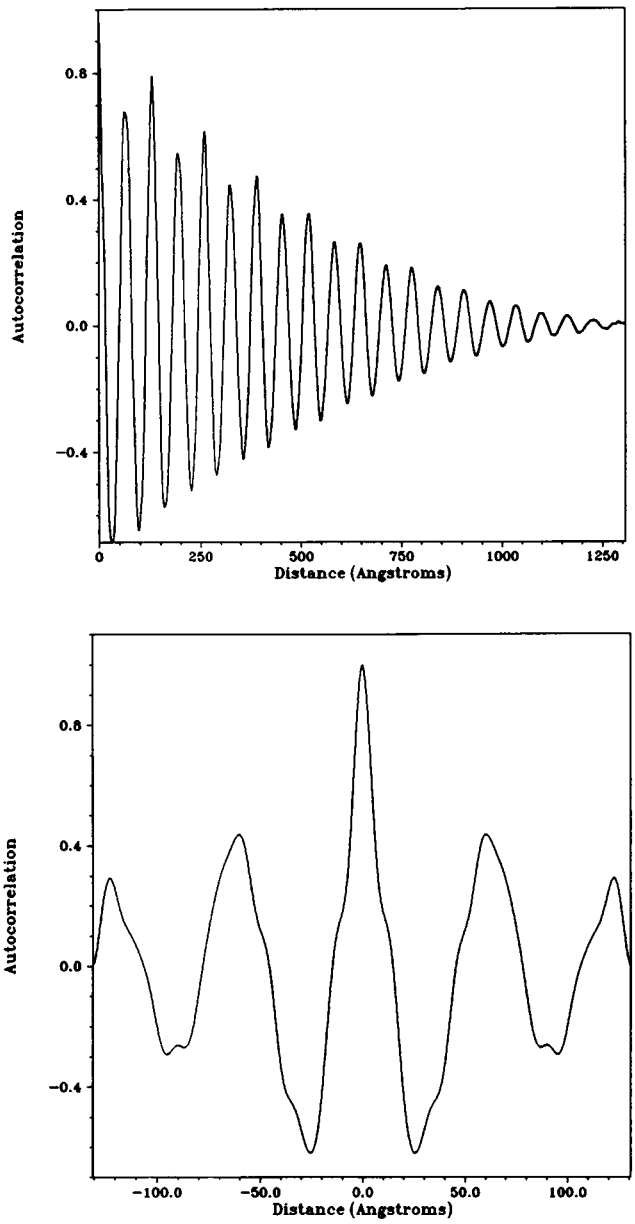

FIGURE 6 Patterson functions. (*a*) The multilayer Patterson function calculated from the diffraction intensities observed at 84% relative humidity and 10°C from an SNM membrane sample without added drug. The repeat distance is ~130 Å. (*b*) The unit cell Patterson function. Note that it goes to zero at the edges.

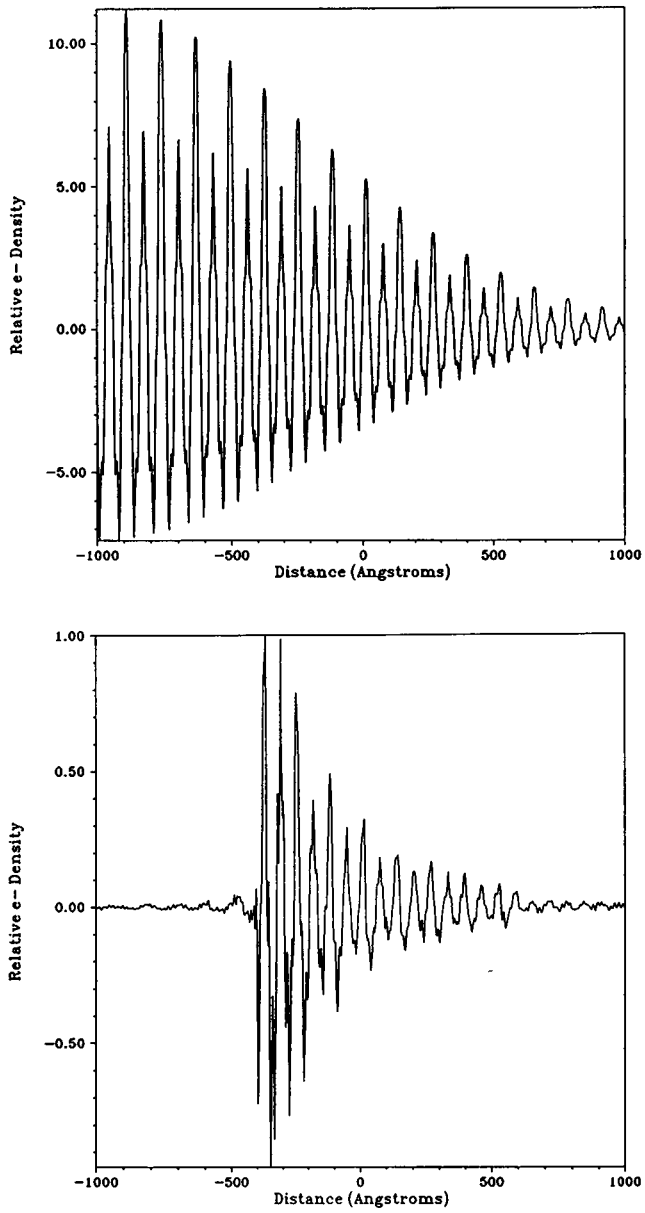

FIGURE 7 Box refinement. (*a*) This trial function was constructed from many repeats of the electron density profile resulting from the direct deconvolution of the unit cell Patterson function. The constructed "multilayer" was then multiplied by a half Gaussian to simulate disorder in the sample. (*b*) The results of a box refinement using the trial function shown in Fig. 6 *a* and a 1000-Å box. The electron density profile is characteristic of a repeating unit containing two membranes. Results using other types of trial functions with boxes from 800 to 1200 Å wide were similar.

density in the upper acyl chain region of the bilayer (Fig. 11 *a*). We believe that this electron density represents the location of the drug in the bilayer. Larger *d* spacings (60–72 Å) were observed for samples made by other than the "spin-dry" method. The quality of diffraction was poorer; at most five orders of diffraction were observed.

Although the differences between the electron density profiles with and without added Ro 15-1788 are small, they are significant. To test the validity of the differences, the integrated intensities of all six orders of diffraction in both the control and Ro 15-1788-added preparations were varied randomly by ±10%. Three sets of random varia-

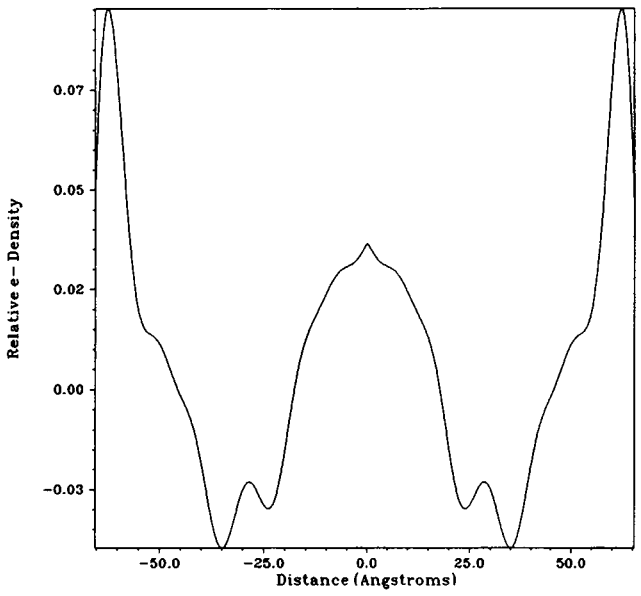

FIGURE 8 Results of deconvolution of the unit cell Patterson function. This symmetrized electron density profile was used for determination of phases. The pointed feature at the center is an artifact due to truncation of the right half of the original profile at $x = 0$ Å and its reversal to form the left half of the profile. The Fourier transform of the profile was calculated and then sampled at intervals of h/d to obtain phases for a centrosymmetric unit cell ($d = 130.7$ Å).

tions were prepared for each set of diffracted intensities; electron density profiles were calculated for all. Then the electron density profile of each control was compared with every electron density profile in which the drug was present. In all cases the characteristic differences of the original electron density profiles were preserved. When the intensities were varied by ±15% and the same procedure was followed, the original differences were still preserved for most of the comparisons. A 10% intensity difference is much greater than any error which may occur during data reduction and analysis; therefore the characteristic differences must be inherent in the data. The structure factor curves for lipids with and without Ro 15-1788 are shown in Fig. 11 *b*. The curves differ significantly, especially in the region where $s \geq 0.09$. This is the region where small changes due to the presence of drug would be likely to appear.

An estimate of the error in the structure factor was made by averaging structure factors calculated from data obtained at two relative humidities at which little structural change in the membranes was indicated. The largest variation of the original structure factor curves from the average was ±2.3%. The largest error in the electron density profiles then must also be ≤2.3%, because the electron density profile is the Fourier transform of the structure factor. The errors in various regions of the electron density profile were estimated by calculating the electron density profile from the average structure factor at the d spacing of the experimental profile and finding the difference between it and the experimentally determined profile. The 5.6% difference between our control and drug-containing samples is admittedly not much greater than the estimated error in the electron density profile; however, the electron density of Ro 15-1788 is relatively low. Our conclusions are based on the results of two experiments at each of three relative humidities; results were clearest at 84% relative humidity.

The structure factors

As part of the swelling study, plots of structure factor vs. h/d were made for the lipid, lipid plus drug, single membrane, and single membrane plus drug data sets. (h is the index of the diffraction order and d is the spacing of the repeating unit.) For the intact membrane data, centrosymmetry is only a close approximation to what the electron micrographs show is a slightly asymmetric structure (see Fig. 3); thus the structure factors for the single membrane unit cell are also approximate. The data for lipid and lipid plus Ro 15-1788 are shown in Fig. 12. All structure factors were found to lie on very closely related curves, regardless of whether they were from lipid or membrane samples, or whether drug had been added. Data for the two-membrane unit cell did not fall upon the same curve as the single-membrane data did. The similarity in the curves for lipids and intact single membranes indicates that the structure seen in our experiments on intact SNM membranes is due mostly to the lipid bilayer, and that any changes due to the protein content of the membrane or to added substances are small. Headgroup separation across the bilayer varied between ~46 Å and ~49 Å, regardless of the type of preparation involved.

Phases for the first, second, and third orders could be assigned unambiguously for both membranes and lipids from the structure factor plots. The structure factors for the third order of diffraction fall on the curve near a node which lies at ~0.0515 $Å^{-1}$. To determine phases for the fourth, fifth, and sixth orders for lipids and the fourth and fifth orders for SNM membranes, all possible phase combinations were used to calculate electron density profiles. All phase combinations which gave physically unreasonable electron density profiles were rejected. Good electron density profiles were characterized by presence of a water space region outside the bilayer, lowest electron density at the center of the methyl trough, a narrow methyl trough, and a relatively flat acyl chain region. However, both phase choices for the fifth order gave acceptable profiles. The following method could not distinguish the better phase choice: two data sets taken from the same sample at different relative humidities

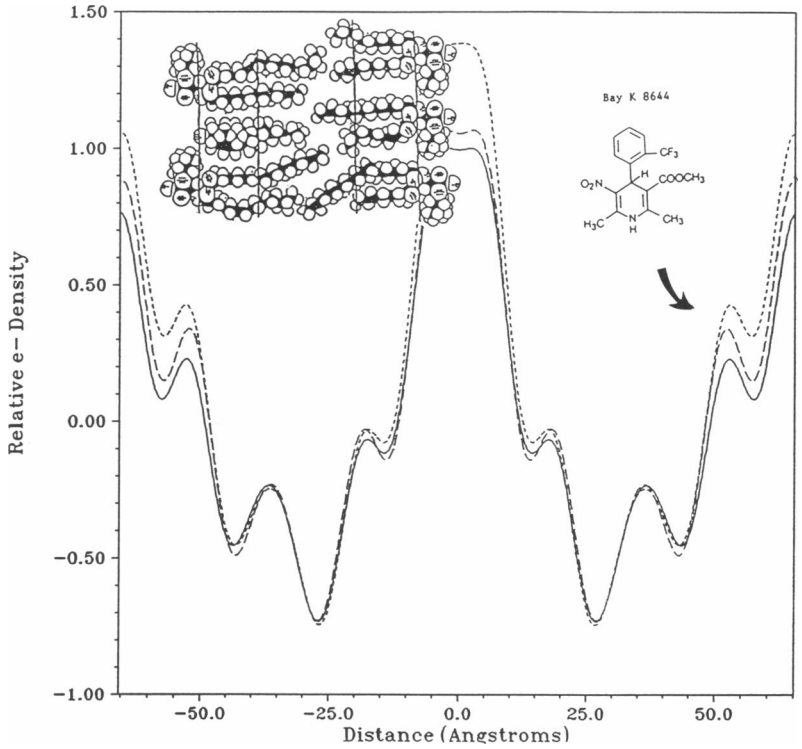

FIGURE 9 Electron density profiles of two-membrane unit cells with and without BAY K 8644. Solid line, control (no drug added), d = 130.7 Å. (*Dashed lines*) BAY K 8644 added at a final concentration of 3 mM (before centrifugation and removal of the supernatant). (*Short dashes*) d = 129.6 Å. (*Long dashes*) d = 130.0 Å. The profiles were calculated by combining experimentally determined intensities with phases obtained by deconvolving the unit cell Patterson functions, calculating the Fourier transforms of the resulting electron density profiles, and sampling the Fourier transforms at intervals of h/d. The methyl trough regions of these profiles were scaled to match; because we cannot measure the intensity at $h = 0$ we have no absolute electron density scale. Experiments on model membranes have shown that the drug does not penetrate to the methyl trough region.

were chosen. Electron density profiles were calculated from each data set using each phase choice for the fifth order. Structure factors were calculated from each electron density profile and then sampled at the periodicities of both data sets. When the squares of the structure factors at those points were compared with the original intensity data, neither phase choice was better than the other at matching either the observed relative intensities of the fourth, fifth, and sixth orders or the change in intensity of the individual orders between the data sets. A second method indicated a probable phase of zero for the fifth order: structure factors were calculated from the electron density profiles derived from two data sets obtained from the same sample at adjacent relative humidities. The structure factors were sampled at the periodicities of both data sets and electron density profiles were calculated. The procedure was repeated using the other phase choice. Then the electron density profiles were compared to see how closely they resembled one another. A positive structure factor for the fifth order gave better results; furthermore, the electron density profiles had a flatter acyl chain region and better-defined headgroup and water space regions. The phases chosen are those represented in the structure factor plot (Fig. 12).

Drug partition coefficients

Partition coefficients (rat SNM membrane/buffer) for the drugs are given in Table 1, as well as the partition coefficients of the DHP drugs in rabbit LSR for comparison. The partition coefficient was corrected for specific binding to the benzodiazepine receptor as follows: the dissociation constant (K_D) for Ro 15-1788 in crude synaptosomal fractions of rat cerebral cortex is 1.0 ± 0.1 nmol/liter; B_{max}, the maximum number of binding sites, is 1.6 ± 0.2 pmol/mg protein (30). These binding data for the synaptosome preparation were used to approximate those for the SNM preparation, which is similar. Our SNM preparation has a phospholipid/protein ratio of ~0.8 μmol phospholipid/mg protein. All the benzodiazepine binding sites were assumed to be occupied by Ro 15-1788. The counts due to specific binding were subtracted from counts due to total binding, and this differ-

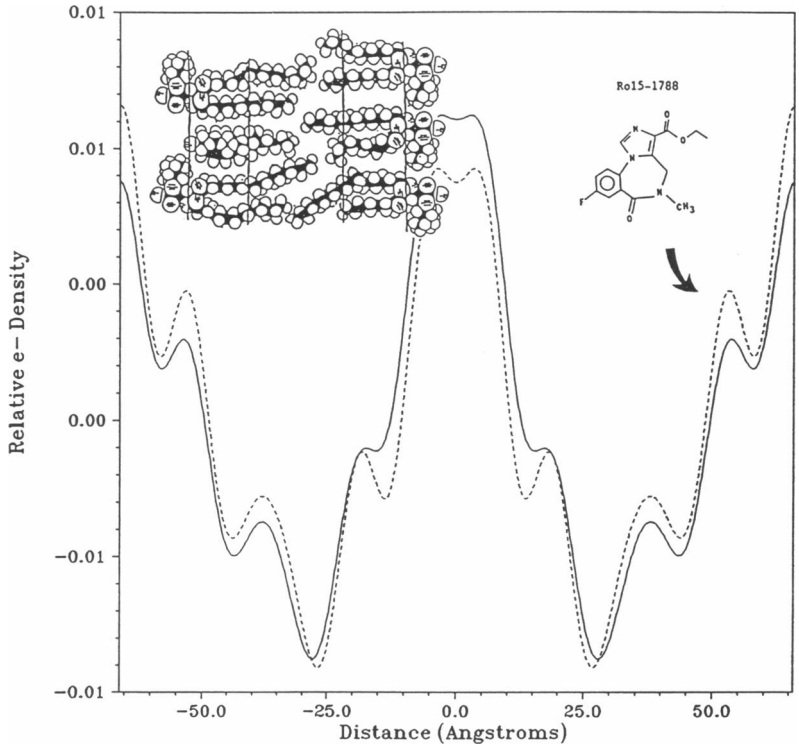

FIGURE 10 Electron density profiles of two-membrane unit cells with and without Ro15-1788. (*Solid line*) Control (no drug added), $d = 132.0$ Å. (*Dashed line*) Ro15-1788 added at a final concentration of 0.6 mM (before centrifugation and removal of the supernatant), $d = 131.6$ Å. The profiles were calculated by combining experimentally determined intensities with phases obtained by deconvolving the unit cell Patterson functions, calculating the Fourier transforms of the resulting electron density profiles, and sampling the Fourier transforms at intervals of h/d. These profiles were scaled using the assumption that the drug causes only a slight perturbation of the electron density profile. The structure factors calculated from the profiles were scaled to each other to minimize differences; then the profiles were recalculated from the scaled structure factors.

ence was used to calculate K_p. Specific binding of DHP drugs was insignificant.

The partition coefficients of drugs in LSR were done by the centrifugation method; all of the partition coefficients in SNM were done by the filtration method. Our previous studies have shown that in LSR, there is no difference between results from the two methods when partition coefficients for DHP drugs are determined (28).

SNM membrane preparations with added drugs

The phase determination procedure described above for the 130-Å unit cell was repeated using data obtained from SNM preparations to which either Ro 15-1788 or BAY K 8644 had been added. The phases determined for the 130-Å unit cell data are shown in Table 2.

BAY K 8644 increased electron density primarily in the outer monolayer of the membrane bilayer from the headgroup region through the acyl chain region (Fig. 9). In cardiac sarcolemmal lipid multibilayers, in the absence of protein, BAY K 8644 partitions into the upper acyl chain region (31). The data for the two-membrane unit cell indicate that Ro 15-1788 partitions into the outer monolayer of the SNM membrane in the upper acyl chain and phospholipid headgroup regions (Fig. 10). It does not reach the inner monolayer. The precise locations of the drugs in the membrane cannot be determined because the resolution (12 Å) is too low.

DISCUSSION

The results reported above represent the first x-ray diffraction study of SNM membranes from cerebral cortical tissue. A diffraction pattern from a dispersion of synaptosomes has been reported by Wilkins et al. (32); synaptosomes arise from the same type of membrane as SNM but are prepared differently (33).

The small amounts of myelin that were apparent in the electron micrographs of the SNM preparations were of concern because myelin diffracts x-rays very well, although an immunoassay for myelin basic protein showed that < 2% by weight of the total membrane in the SNM

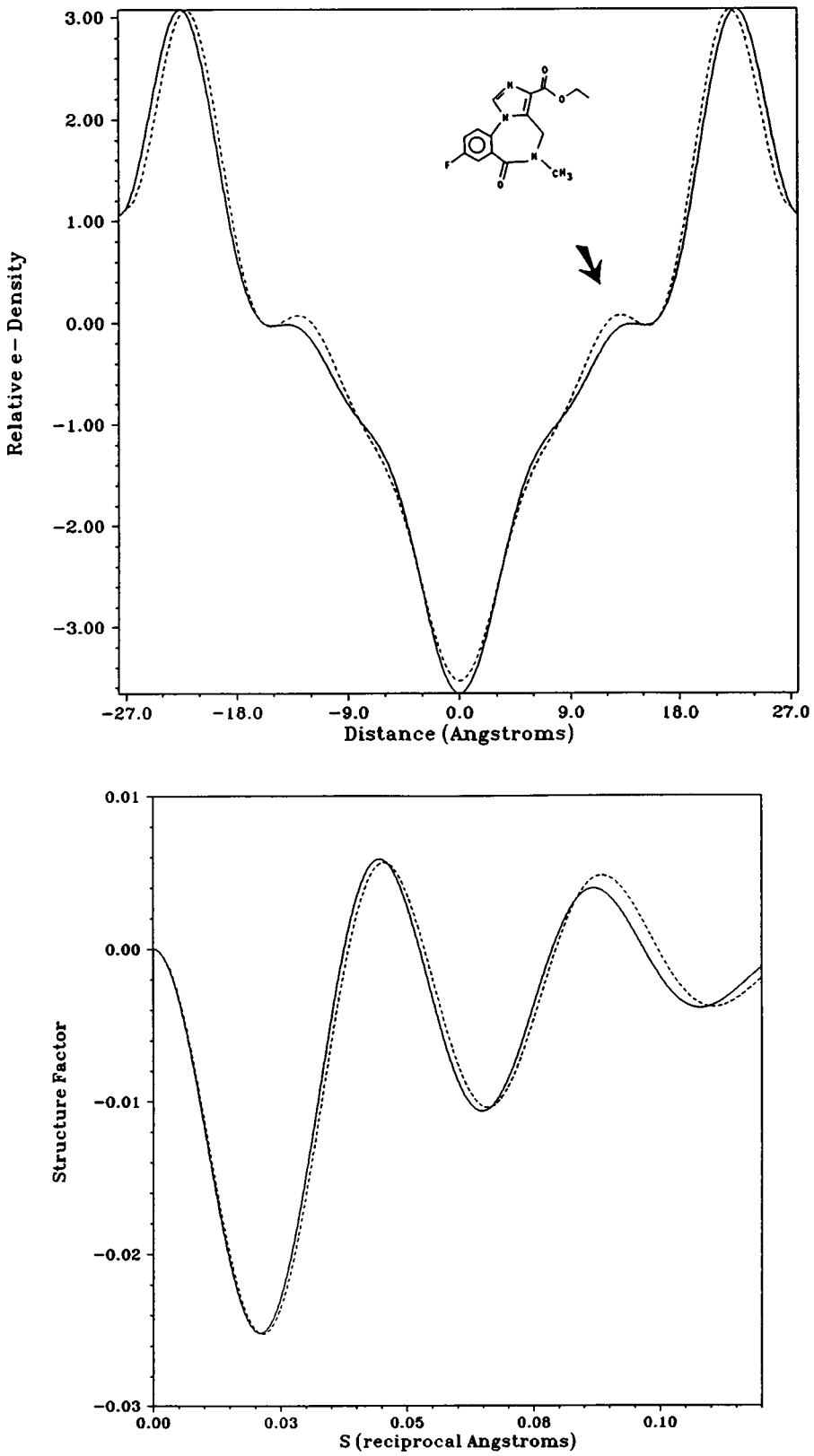

FIGURE 11 Ro 15-1788 in extracted SNM membrane lipids. (*a*) Comparison of electron density profiles of spin-dried rat SNM lipids at 84% relative humidity and 10.0°C. (*Solid curve*) No drug added, $d = 55.3$ Å; (*Dashed curve*) 1 mol Ro15-1788:30 mol lipid, $d = 54.0$ Å. The arrow indicates an increase in electron density. (*b*) Structure factors calculated from the electron density profiles in Fig. 11 *a*. (*Solid curve*) No drug added, $d = 55.3$ Å; (*dashed curve*) 1 mol Ro 15-1788:30 mol lipid, $d = 54.0$ Å. The differences are greatest in the region, where $s \geq 0.09$, the region corresponding to the location of sixth order of diffraction.

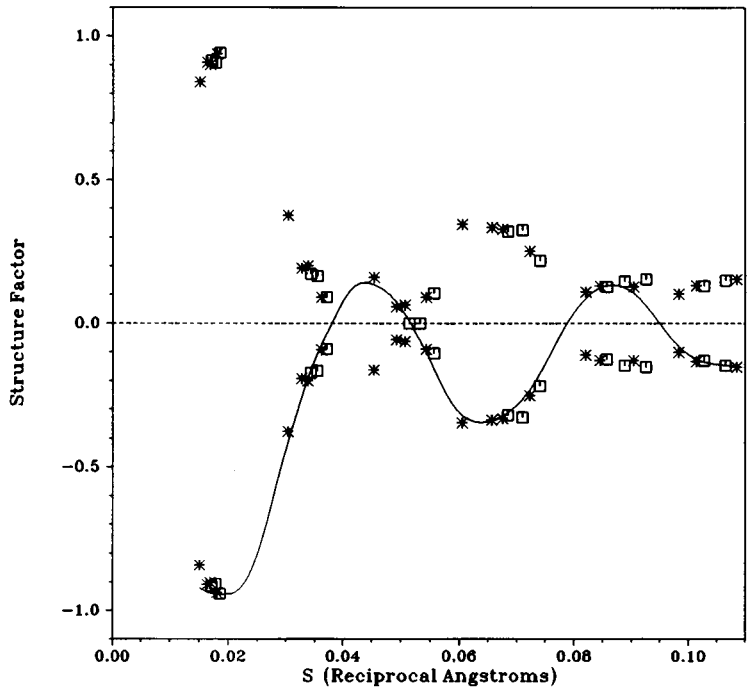

FIGURE 12 Experimental structure factor curve. Structure factors for SNM extracted lipids without added drug (*stars*), and for lipids with added Ro 15-1788 (*boxes*). The drug/lipid mole ratio is 1:30. The curve shown is a spline fit to the control data (*stars*) with the phases chosen as described in the text. The opposite phase choice for the fifth order (negative structure factor) also produced a reasonable electron density profile (see Results). Data for lipids with added drug are shown to illustrate that the curves are similar, but do not coincide.

preparation is myelin. The *d* spacing for myelin in intact nerve fibers is 150–180 Å, corresponding to the thickness of two membranes (24). At low relative humidity, the *d* spacing of our SNM preparation is only 130 Å. None of our SNM preparations exhibited such a large *d* spacing at high relative humidity. Sedzik et al. obtained a *d* spacing of 74–76 Å for preparations of isolated myelin (11). This *d* spacing is comparable to that calculated for the SNM preparations. A weak ring of Bragg-like diffraction corresponding to a *d* spacing of 76 Å appeared in diffraction from dispersions of vesicles. The ring would be due to multilamellar vesicles or to multilamellar fragments of membrane, possibly myelin. Because of its innate order, a small amount of multilamellar material in a suspension of vesicles would diffract much more strongly than unilamellar vesicles at a similar concentration. Diffraction results using multilayer, oriented samples of myelin-free shiverer mouse SNM were indistinguishable from those from rat SNM. Therefore, diffraction due to myelin, if any, is unlikely to affect significantly the diffraction pattern from our SNM multilayer samples.

TABLE 1 Partition coefficients of imidazobenzodiazepine and dihydropyridine drugs

Drug	K_p(SNM lipid extract)	K_p(LSR*)
BAY K 8644	1,093 (±380)‡	11,000 (31)
Nimodipine	1,100 (±220)‡	5,000 (7, 28)
Ro 15-1788	37 (±47)‡§	17 (±17)‡

*LSR = rabbit light sarcoplasmic reticulum.
‡This work. Numbers in parentheses are standard deviations.
§Grand mean of 18 determinations (n = 3).

TABLE 2 Phases for data from the two-member unit cell

	Order										
Sample type	1	2	3	4	5	6	7	8	9	10	11
Controls	0	0	0	0	0	0	0	0	π	π	π
BAY K 8644	0	0	0	0	0	0	0	0	π	π	π
Ro 15-1788	π	0	0	0	0	0	0	0	π	π	π

Structure of SNM membranes

We were unable to determine phases for the single-membrane unit cell data by method of Blaurock and King (13) because we obtained only low-resolution results from diffraction experiments on dispersions of SNM mem-

brane vesicles. Nevertheless, assumption of centrosymmetry gives a close approximation of the structure (see Results) and is useful for comparisons among data sets. The electron density profiles (calculated assuming centrosymmetry of the membrane) and diffraction patterns of SNM are typical of those of biological membranes containing protein, with d spacings in the range 71–87 Å, depending on the hydration state of the membrane.

Analysis of the data for the 130-Å unit cell yields a unit cell containing two membranes (Fig. 9); the individual membranes are somewhat asymmetric. The outer surface of the bilayer contains more protein and therefore has a lower electron density than the inner surface. This difference in protein content is confirmed by high-magnification electron micrographs of SNM; the outer monolayer of the membrane is more densely stained than the inner monolayer (Fig. 3). When the relative humidity is lowered sufficiently, each collapsed membrane vesicle forms a single unit cell containing two back-to-back membranes. Thus the unit cell is likely to be centrosymmetric.

Data for the single- and double-membrane unit cells do not fall on the same structure factor squared curve. This is further confirmation that the membranes are stacked in groups of two and not stacked randomly. In the case of random stacking, the new two-membrane unit cell at low relative humidities would not appear, and the squared structure factors would continue to lie on the same curve. The change in diffraction pattern occurs suddenly within a narrow range of relative humidities and is completely reversible. We explain this sudden d space change as follows: at higher hydration states, water obscures the regular stacking pattern of the asymmetric membranes by "diluting" the protein, glycosylation, etc. present at the outer surfaces of the membranes so that the unit cell represents the averaged structures of the asymmetric single membrane. Removal of enough water results in an electron density contrast that causes these surface features to affect the diffraction pattern, requiring a new, two-membrane repeating unit which is centrosymmetric. The single membrane, in which this contrast is low, is unlikely to be highly asymmetric; if it were, the unit cell at higher hydration states would probably contain two membranes.

Molecular interaction of drugs with SNM membranes and membrane lipids

Lipid extracts

The presence of protein in the membrane is a source of some disorder in the membrane multilayer stack; various kinds of protein can also interact with the drug, specifically or nonspecifically. Control of the exact concentration of the drug in the membrane multilayer diffraction sample is also impossible, as the supernatant, which contains some of the added drug, is removed after centrifugation of the diffraction sample. Extracted lipids are a simpler system, and the results are more easily interpretable. Furthermore, because the lipid bilayer must be centrosymmetric, accurate phasing is possible. The drug concentration can be precisely controlled by using the "spin-dry" technique (22), in which all volatile fluids are dried off under vacuum during centrifugation. Afterward, the multibilayer, containing all of the added drug, is partially rehydrated. This technique is too harsh for intact membranes because it can cause phase separation. For these reasons, we conducted diffraction experiments on lipids extracted from SNM membranes in the hope of clarifying the interactions of the drugs with intact membrane.

In the diffraction experiments on extracted lipids, an electron density increase appeared in the upper acyl chain region of the electron density profile of the lipids with added Ro 15-1788 (*arrow*, Fig. 11). We attribute this electron density to the presence of the drug. Only a small electron density increase would be expected because Ro 15-1788 has only a ring system and a single fluorine atom to raise its electron density relative to the bilayer and increase the contrast. Ro 15-1788 crystallizes in a tetragonal unit cell of 2697 $Å^3$ vol, $Z = 8$ (34). From the crystal data and chemical formula, its electron density is 0.469 e-$Å^{-3}$. The electron densities of the headgroup, glycerol backbone, and acyl chain regions of a pure DPPC bilayer are 0.46, 0.42, and 0.26 e-$Å^{-3}$, respectively (35). These electron densities roughly approximate those of the extracted lipid bilayer. If the drug is located in the headgroup region and occupies approximately the space of a lipid molecule, then it may have low contrast in that region, and also possibly in the glycerol backbone region. Electron density contrast due to Ro 15-1788 located in the acyl chain region would be more likely to show up, and indeed, that is what appears. The presence of the drug appears to widen the methyl trough region somewhat, indicating some disordering of the acyl chains. Our results show that the drug binds nonspecifically in the upper acyl chain region in the absence of protein, but the headgroup and glycerol backbone regions are not ruled out.

Partition coefficients and drug interaction with intact SNM membranes

When BAY K 8644 is added to the SNM preparation, it increases the electron density primarily in the outer monolayer of the membrane. BAY K 8644 appears to interact at the headgroup region through the upper acyl chain region (Fig. 9), probably with the protein located there. Some BAY K 8644 penetrates to the inner monolayer of the membrane. BAY K 8644 seems to impart

order to the diffraction sample and often delays phase separation; our highest quality data on the 130-Å unit cell were obtained from samples containing BAY K 8644. In intact membrane, Ro 15-1788 interacts with the headgroup region, but unlike BAY K 8644, it does not appear to reach the inner monolayer of the membrane at all (Fig. 10). This behavior indicates a surface interaction with the membrane protein. Our preliminary data show that the partition coefficient of Ro 15-1788 in intact SNM membranes is somewhat higher than in SNM lipid extracts. The higher partition coefficient in the presence of protein supports a nonspecific surface interaction with membrane protein. The decrease in electron density at the center of the vesicle in the drug-containing sample relative to the control is probably due to the smaller water space in the control. These results are preliminary; the contrast of these drugs with the membrane in x-ray diffraction experiments is low. Analogous neutron diffraction experiments using deuterated drugs, which will provide better contrast, are planned.

In Table 1 membrane/buffer partition coefficients of DHP's are given for LSR as well as for SNM. In LSR, the partition coefficients of the DHP's are increased approximately threefold over those in SNM. The reason for this increase might be the differences in cholesterol content of the two types of membrane. We found that the cholesterol/phospholipid mole ratio in our lipid extracts of rat brain SNM membranes was 0.7; in extracts of rabbit skeletal muscle LSR the mole ratio was only 0.06. Cholesterol positions itself in the membrane lipids in the region of the hydrocarbon core which is just below the glycerol backbone, with the cholesterol molecule oriented parallel to the hydrocarbon chains (36). A high concentration of cholesterol may tend to exclude drugs from the upper portion of the acyl chain region, which is the area into which the DHP's normally partition. When the DHP calcium channel antagonist nimodipine was introduced into dioleolylphosphatidylcholine (DOPC) lipid bilayers containing 0.30 mol of cholesterol per mole of phospholipid, the partition coefficient of the drug was reduced to half its value in DOPC bilayers containing no cholesterol. Higher cholesterol concentrations produced even further lowering of the partition coefficient. By this reasoning the partition coefficients of DHP's in SNM would be lower than those in LSR, if the interaction is with the hydrocarbon core of the membrane bilayer.

The imidazobenzodiazepines, which appear to interact with the membrane surface and headgroup region in intact membrane, are less affected by the higher cholesterol content of SNM.

Rhodes et al. (37) calculated the kinetics of approach of DHP drugs to their binding site on the Ca^{2+} channel in cardiac sarcolemmal membrane. Two models were used. The first was direct approach of the drug to its binding site through the aqueous medium. The second was approach of the drug through the membrane, a two-step mechanism in which the drug first partitions somewhere into the membrane bilayer and then diffuses laterally to its binding site. The first model requires that the binding site be in contact with the aqueous medium. In the second model, the binding site must be located at the preferred nonspecific binding depth of the drug in the membrane. Otherwise the drug will not contact its binding site during diffusion (28). The calculated diffusion-limited rate of approach for the membrane approach model was found to be three orders of magnitude greater than that for the aqueous approach model.

It is likely that the membrane approach to the binding site is an efficient one for both the imidazobenzodiazepines and the dihydropyridines. It appears that Ro 15-1788 is located in the phospholipid headgroup region through the upper acyl chain region in the intact membrane and possibly also in the extracted lipid bilayer. We expect the benzodiazepine receptor site to be located on the $GABA_A$/benzodiazepine receptor complex somewhere near the surface of the membrane bilayer, so that the drug diffusing through the hydrophilic region of the membrane would eventually come into contact with its specific binding site on the receptor protein.

Summary and Implications of the Work

Electron microscopy and x-ray diffraction showed that the SNM membrane is somewhat asymmetric. X-Ray diffraction experiments indicated that the imidazobenzodiazepine Ro 15-1788 and the DHP BAY K 8644 partition into the intact membrane in the region from the headgroup through the upper part of the acyl chains. Both drugs appear to be located primarily in the outer monolayer of the membrane; Ro 15-1788 appears not to enter the inner monolayer at all; it interacts strongly with the membrane protein in intact SNM membrane. These experiments are preliminary to planned experiments using neutron diffraction with deuterated drugs for better contrast. Partition coefficients for DHP drugs are approximately fivefold higher in LSR than in SNM. This difference is possibly attributable to the higher cholesterol content of SNM compared with LSR. Both the DHP's and imidazobenzodiazepines are likely to approach their specific binding sites on membrane receptor proteins via a two-step membrane pathway rather than by an aqueous route. Neutron scattering experiments have shown that ethanol partitions into LSR primarily throughout the aqueous region of the membrane (the headgroup and glycerol backbone region) and is excluded from the hydrocarbon core (38). Ro 15-1788 partitions into the aqueous region of the SNM membrane. The imidazoben-

zodiazepines, then, would be likely to interact directly with ethanol and with their specific binding sites on the receptor protein in the headgroup/glycerol backbone region of the membrane. This hypothesis is consistent with the antagonism by Ro 15-4513 of some of the behavioral intoxicating effects of acute ethanol administration, and of its selective antagonism of ethanol-related increase in GABA-mediated chloride flux (2, 3).

We are grateful to Dr. Elisa Barbarese for the gift of shiverer mice, and to Mr. Christopher Barry for conducting the immunoassay for myelin basic protein. We should like to thank Ms. Yvonne Vant Erve, Ms. Lisa Ganley, and Ms. Lydia Shajenko for performing the partition coefficient experiments, and Ms. Lavinia Muncy and Dr. T. J. MacAlister for carrying out the electron microscopy work. We are grateful to Dr. Peter Sorter of Hoffmann-La Roche, Inc., for providing Ro 15-1788 and Ro 15-4513. Dr. Roger Meyer provided continuing helpful discussions on relating our results to clinical questions.

This work was supported by National Institute on Alcohol Abuse and Alcoholism grants #P50-AA03510 and #T32-AA0720, Heublein, Inc., and by a grant from the American Health Assistance Foundation. The work was carried out in the Alcohol Research Center and the Biomolecular Structure Analysis Center. Dr. Herbette is an Established Investigator of the American Heart Association. We should like to thank the staff of the Structure Center for their dedication in keeping the facilities in optimal running condition. The Structure Center acknowledges support from the State of Connecticut Department of Higher Education's High Technology Programs, from RJR Nabisco, Inc., and core support from National Institute of Health HL-33026.

Received for publication 23 August 1988 and in final form 4 April 1990.

REFERENCES

1. Hollingsworth, B., E. T. McNeal, J. L. Burton, R. J. Williams, J. W. Daly, and C. R. Creveling. 1985. Biochemical characterization of a filtered synaptoneurosome preparation from guinea pig cerebral cortex: cyclic adenosine 3':5'-monophosphate-generating systems, receptors, and enzymes. *J. Neurosci.* 5:2240–2253.
2. Suzdak, P. D., R. D. Schwartz, P. Skolnick, and S. M. Paul. 1986. Ethanol stimulates γ-aminobutyric acid receptor-mediated chloride transport in rat brain synaptoneurosomes. *Proc. Natl. Acad. Sci. USA.* 83:4071–4075.
3. Suzdak, P. D., J. R. Glowa, J. N. Crawley, R. D. Schwartz, P. Skolnick, and S. M. Paul. 1986. A selective imidazobenzodiazepine antagonist of ethanol in the rat. *Science (Wash. DC).* 234:1243–1247.
4. Littleton, J. M., and H. J. Little. 1988. Dihydropyridine-sensitive $Ca2^+$ channels in brain are involved in the central nervous system hyperexcitability associated with alcohol withdrawal states. *Ann. N.Y. Acad. Sci.* 522:199–202.
5. Dolin, S., H. Little, M. Hudspith, C. Pagonis, and J. Littleton. 1987. Increased dihydropyridine-sensitive calcium channels in rat brain may underlie ethanol physical dependence. *Neuropharmacology.* 26:275–279.
6. Little, H. J., S. Dolin, and M. J. Halsey. 1986. Calcium channel antagonists decrease ethanol withdrawal syndrome. *Life Sci.* 39:2059–2065.
7. Herbette, L. G., D. W. Chester, and D. G. Rhodes. 1986. Structural analysis of drug molecules in biological membranes. *Biophys. J.* 49:91–94.
8. Herbette, L. G., T. MacAlister, T. F. Ashavaid, and R. A. Colvin. 1985. Structure-function studies of canine cardiac sarcolemmal membranes. II. Structural organization of the sarcolemmal membrane as determined by electron microscopy and lamellar x-ray diffraction. *Biochim. Biophys. Acta.* 812:609–623.
9. Herbette, L. G., J. Marquardt, A. Scarpa, and J. K. Blasie. 1977. A direct analysis of lamellar x-ray diffraction from hydrated oriented multilayers of fully functional sarcoplasmic reticulum. *Biophys. J.* 20:245–272.
10. Blaurock, A. E. 1986. X-Ray and neutron diffraction by membranes: how great is the potential for defining the molecular interactions? *In* Progress in Protein-Lipid Interaction. Watts and de Pont, editors. 2:2–43.
11. Sedzik, J., A. D. Toews, A. E. Blaurock, and P. Morell. 1984. Resistance to disruption of multilamellar fragments of central nervous system myelin. *J. Neurochem.* 43(5):1415–1420.
12. Kirschner, D. A., and R. L. Sidman. 1976. X-Ray diffraction study of myelin structure in immature and mutant mice. *Biochim. Biophys. Acta.* 448:73–87.
13. Blaurock, A. E., and G. I. King. 1977. Asymmetric structure of the purple membrane. *Science (Wash. DC).* 186:1101–1104.
14. Ross, M. J., M. W. Klymkowsky, D. A. Agard, and R. M. Stroud. 1977. Structural studies of a membrane-bound acetylcholine receptor from *Torpedo californica. J. Mol. Biol.* 116:635–659.
15. Lowry, O. H., N. J. Rosebrough, A. L. Farr, and R. J. Randall. 1951. Protein determination with the phenol reagent. *J. Biol. Chem.* 193:265–275.
16. Chen, P. S., T. Y. Toribara, and H. Warner. 1956. Microdetermination of phosphorus. *Analytical Chem.* 28:1756–1758.
17. Blasie, J. K., C. R. Worthington, and M. M. Dewey. 1969. Molecular localization of frog retinal receptor photopigment by electron microscopy and low-angle x-ray diffraction. *J. Mol. Biol.* 39:407–416.
18. Folch, J., M. Lees, and G. H. Sloane Stanley. 1957. A simple method for the isolation and purification of total lipides from animal tissues. *J. Biol. Chem.* 226:497–509.
19. Heider, J. G., and R. L. Boyett. 1978. The picomole determination of free and total cholesterol in cells in culture. *J. Lipid Res.* 19:514–518.
20. Chester, D. W., M. E. Tourtelotte, D. L. Melchior, and A. H. Romano. 1986. The influence of fatty acid modulation of bilayer physical state on cellular and membrane structure and function. *Biochim. Biophys. Acta.* 860:383–398.
21. Bangham, A. D., M. M. Standish, and J. C. Watkins. 1965. Diffusion of univalent ions across the lamellae of swollen phospholipids. *J. Mol. Biol.* 13:238–252.
22. Chester, D. W., L. G. Herbette, R. P. Mason, A. F. Joslyn, D. J. Triggle, and D. E. Koppel. 1987. Diffusion of dihydropyridine calcium channel antagonists in cardiac sarcolemmal lipid multilayers. *Biophys. J.* 52:1021–1030.
23. Clark, N. A., K. J. Rothschild, D. A. Luippold, and B. A. Simon. 1980. Surface-induced lamellar orientation of multibilayer membrane arrays—theoretical analysis and a new method with application to purple membrane fragments. *Biophys. J.* 31:65–96.
24. Moody, M. F. 1963. X-Ray diffraction pattern of nerve myelin: a method for determining the phases. *Science (Wash. DC).* 142: 1173–1174.

25. Stroud, R. M., and D. A. Agard. 1979. Structure determination of asymmetric membrane profiles using an iterative Fourier method. *Biophys. J.* 25:495–512.

26. Lesslauer, W., and J. K. Blasie. 1972. Direct determination of the structure of barium stearate multilayers by x-ray diffraction. *Biophys. J.* 12:175–190.

27. Schwartz, S., J. E. Cain, E. A. Dratz, and J. K. Blasie. 1975. An analysis of lamellar x-ray diffraction from disordered membrane multilayers with application to data from retinal rod outer segments. *Biophys. J.* 15:1201–1233.

28. Herbette, L. G., Y. M. H. Vant Erve, and D. G. Rhodes. 1989. Interaction of 1,4-dihydropyridine calcium channel antagonists with biological membranes: Lipid bilayer partitioning could occur before drug binding to receptors. *J. Mol. Cell. Cardiol.* 21:187–201.

29. Barbarese, E., M. L. Nielson, and J. H. Carson. 1983. The effect of the shiver mutation on myelin basic protein expression in homozygous and heterozygous mouse brain. *J. Neurochem.* 40:1680–1686.

30. Mohler, H., W. P. Burkard, H. H. Keller, J. G. Richards, and W. Haefely. 1981. Benzodiazepine antagonist Ro 15-1788: Binding characteristics and interaction with drug-induced changes in dopamine turnover and cerebellar cGMP levels. *J. Neurochem.* 37:714–722.

31. Mason, R. P., G. E. Gonye, D. W. Chester, and L. G. Herbette. 1989. Partitioning and location of BAY K 8644, 1,4-dihydropyridine calcium channel agonist, in model and biological lipid membranes. *Biophys. J.* 55:769–778.

32. Wilkins, M. H. F., A. E. Blaurock, and D. M. Engelman. 1971. Bilayer structure in membranes. *Nature New Biol.* 230:72–76.

33. Whittaker, V. P. 1965. The application of subcellular fractionation techniques to the study of brain function. *Prog. Biophys. Mol. Biol.* 15:39–96.

34. Codding, P. W., and A. K. S. Muir. 1985. Molecular structure of Ro 15-1788 and a model for the binding of benzodiazepine receptor ligands. *Mol. Pharmacol.* 28:178–184.

35. Trumbore, M., D. W. Chester, J. Moring, D. Rhodes, and L. G. Herbette. 1988. Structure and location of amiodarone in a membrane bilayer as determined by molecular mechanics and quantitative x-ray diffraction. *Biophys. J.* 54:535–543.

36. Yeagle, P. L. 1985. Cholesterol and the cell membrane. *Biochim. Biophys. Acta* 822:267–287.

37. Rhodes, D. G., J. G. Sarmiento, and L. G. Herbette. 1985. Kinetics of binding of membrane-active drugs to receptor sites. Diffusion-limited rates for a membrane bilayer approach of 1,4-dihydropyridine calcium channel antagonists to their active site. *Mol. Pharmacol.* 27:612–623.

38. Herbette, L., C. A. Napolitano, F. C. Messineo, and A. M. Katz. 1985. Interaction of amphiphilic molecules with biological membranes. A model for nonspecific and specific drug effects with membranes. *Adv. Myocardiol.* 5:333–346.